J Fluoresc (2008) 18:93–100
DOI 10.1007/s10895-007-0241-x

ORIGINAL PAPER

Fluorescence Spectral Properties of Rhodamine 6G at the Silica/Water Interface

Zhe Chen · Yao-Ji Tang · Tang-Tang Xie · Ying Chen · Yao-Qun Li

Received: 24 May 2007 / Accepted: 14 August 2007 / Published online: 25 September 2007
© Springer Science + Business Media, LLC 2007

Abstract In this work, total internal reflection synchronous fluorescence spectroscopy (TIRSF) is applied successfully to investigate rhodamine 6G (R6G) at the silica/water interface. In comparison with the bulk spectra, 5 nm red shift is observed in the interface spectra, which is mainly due to the limitation of freedom of rotational movement of R6G molecules at the interface. The increase of R6G concentration induces the self-quenching of adsorbate at the interface. The dependence of interfacial fluorescence on the acidity and ionic strength was studied. Both the acidity and ionic strength affect the adsorptive behaviors of R6G at the silica/water interface.

Keywords TIRSF · R6G · Silica/water interface

Introduction

Of particular interest in interface analysis is the optical characteristic of molecules affected by their physical and chemical environment [1–4]. In last few decades, many efforts were focused on photophysics and photochemistry of interfaces [5–11]. On the other hand, many species, especially dyes, were examined on materials [12], ordered supramolecular assemblies [13] in attempt to understand the phenomena that happen at interfaces. However, the behavior of the asymmetric forces acting on molecules is more complex and inhomogenous at the interface than in the bulk phase, which is both qualitatively and quantitatively well known. One of the key problems in the investigation of the interface is the adsorption of molecules, which reflects the weak interaction between environment and molecules [14, 15].

As a common cationic dye, rhodamine 6G (R6G, Fig. 1) has been employed to observe phenomena at the interface on the physical and chemical aspects for a long time [1, 2, 4–7]. López Arbeloa et al. [16] probed the orientation of R6G in the clay by using florescence polarization. Brennan et al. [17] applied time-resolved fluorescence anisotropy approach to measure the surface coverage of SiO_2 in the bulk solution. However, there are only a few tools available for probing surface without disturbance from the bulk phase or probing interface origins directly.

In order to study molecules at silica/water interface with fluorescence approaches, it is necessary to distinguish the interface-originated signals with those from a large overwhelming number of molecules in the bulk solution. Total internal reflection fluorescence (TIRF) spectroscopy is chosen in this study because it is of interface-specific and can be easily applied to in situ observation at an interface [11, 18–20]. Synchronous fluorescence spectroscopy has been shown to give narrow and simple spectra [21–24]. Unlike conventional fluorescence excitation and emission spectra, a synchronous fluorescence spectrum is taken as a combined function of excitation and emission wavelengths. The simplest synchronous scanning technique maintains a constant-wavelength difference ($\Delta\lambda$) between emission and excitation wavelengths during the acquisition of a spectrum. The combination of TIRF and synchronous scanning technique has been suggested in a previous paper [25].

The goal of this work is to investigate the adsorption of R6G on silica/water interface, to discuss the causes for the interfacial fluorescence behaviors, and to provide a novel perspective to recognize surface-active molecules. In this

Z. Chen · Y.-J. Tang · T.-T. Xie · Y. Chen · Y.-Q. Li (✉)
Department of Chemistry and The Key Laboratory of Analytical Sciences of the Ministry of Education, College of Chemistry and Chemical Engineering, Xiamen University,
Xiamen 361005, China
e-mail: yqlig@xmu.edu.cn

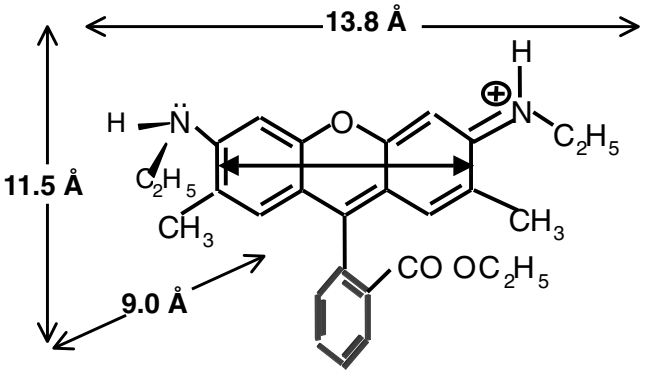

Fig. 1 Sketch plot of the structure of Rhodamine 6G

work, total internal reflection synchronous fluorescence spectroscopy (TIRSF) is applied successfully to measure rhodamine 6G (R6G) at the silica/water interface. The mechanism of the spectral red shift of R6G at the interface is proposed. The effects of concentrations, solution acidity and ionic strength on fluorescent intensity are studied.

Experimental section

Materials Rhodamine 6G (Shanghai Reagent Inc.) was of analytical grade and used without further purification. For the experiments on acidity effects, 1.0 M HCl was used to prepare serial solutions of R6G with different pH. The ionic strength of the solution was adjusted with 2.0 M NaCl. Other reagents were of analytical grade. All solutions were prepared with deionized water.

Hydrophobic silica slice was processed by dichlorodimethylsilane ($(CH_3)_2SiCl_2$).

Apparatus TIRF measurement and bulk phase measurements were carried out by a home-made multifunctional spectrofluorimeter as previously described [22, 23, 26]. It was equipped with a 150 W xenon lamp and the slit bandpasses of excitation and emission monochromators were set at 5 nm. The bulk observation was performed with the spectrofluorimeter at regular detection manner (10 mm×10 mm cell). For TIRF measurement, a cylindrical prism was attached to a sample cell consisting with two sandwiched silica slices (20 mm×20 mm) and gaskets used as spacer to make TIRF sample cell (Fig. 2). Glycerol was used to agglutinate the slice and prism. Passing a cylindrical prism, a beam of light went from optically denser medium (silica, refractive index, n_1=1.46) to the optically thinner medium (water, refractive index, n_2=1.33) at a fixed incidence angle of 70°, which is greater than the critical angle (66°) in silica/water interface, the light undergoes total internal reflection. The evanescent wave excites the fluorophores of molecules at the interface

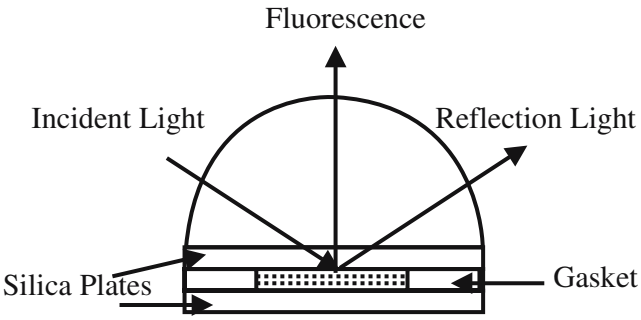

Fig. 2 Schematic drawing of TIRF cell

region. Combining synchronous fluorescence technique with a Δλ of 24 nm, thus, interfacial synchronous fluorescence spectra are obtained.

The measurement at toluene/water interface refers to Watarai et al. [39].

Results and discussion

Interface-originated fluorescence of R6G

The fluorescence spectra of R6G obtained from silica/water and bulk phase at 1.0×10^{-7} M are shown on Fig. 3. The overlap between the excitation and emission spectra is attributed to the low energy transitions between the ground and the first excited states (S_0-S_1) of R6G. Researchers usually select an excitation wavelength that can avoid the interference of Rayleigh scattering on the spectra at the sacrifice of fluorescence intensity or obtain incomplete

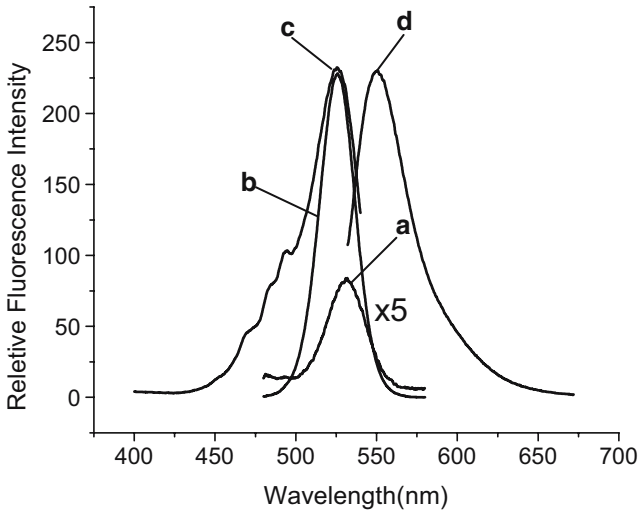

Fig. 3 The fluorescence spectra of R6G in different host environments, *a* synchronous spectrum (Δλ=24 nm) at silica/water interface (the intensity amplified fivefold), *b* synchronous spectrum (Δλ=24 nm) in aqueous solution, *c* excitation and *d* emission spectra in aqueous solution. [R6G]=1.0×10^{-7} M, PBS 7.4

excitation/emission spectra [1, 5]. In this study, the synchronous scanning technique was applied to overcome the shortcoming. A constant-wavelength difference ($\Delta\lambda$= 24 nm) for synchronous scanning was chosen, which was equal to the Stokes' shift of R6G.

As shown in Fig. 3, the wavelength of the peak maximum is red-shifted from 525 nm (Fig. 3*b*) in aqueous bulk solution to 530 nm (Fig. 3*a*) at the silica/water interface with water phase R6G concentration of 1.0×10^{-7} M. To investigate the causes of the red shift, the same experiments were carried out (Table 1) at the toluene/water and hydrophobic silica/water interface. The red shifts were also observed in both measurements. However, no aggregation was found at interfaces at this concentration.

Previous studies rationalized the bathochromic shift of the emission maxima of molecules on substrates in several ways. The first assumption for the cause is the effect of the environment of dye molecules, such as changes in polarity or polarizability [27], as the general solvent effects are determined by the polarizability of solvent or fluorophore. The fluorophores present diverse spectral features in different environments. Interdigitated effect of the long alkyl chains between adjacent layers in the Langmuir–Blodgett films alters the structure of porphyrin aggregates [28]. The fluorescence spectra of FITC-labeled colloidal silica spheres show a concentration-dependence red shift, which comes from the lower surface polarity for the interactions between neighboring molecules [27]. An alternative explanation for the red shift could be the formation of aggregates [29]. The exciton theory [30], a molecular quantum mechanical theory based on monomer dipole–dipole interaction in the aggregates, illustrates the spectroscopic characteristics of dimers. Long displaced coplanar dimers with a tilt angle $\theta<54.7°$ have active absorption and fluorescence J bands [29], which appear at lower energy than the monomeric fluorescent band. The short displaced coplanar dimers with a tilt angle $\theta>54.7°$ undergo the transition to the highest excited state in absorption and the deactivation to the ground state with nonfluorescing. The inner filter effects in high dye concentration samples could be the third factor for obviously red shift [31]. The fourth hypothesis is that the entrapped molecules in the matrix are constrained by the corresponding surface. The high orientation of molecules in the surface can cause new configuration and dynamic behavior quite different from those in homogeneous solution. Not only the powdered or porous materials, but also polymeric block or monolayer supporters can impose the dye molecules in contradistinction to fluid environment [1, 29, 32, 33]. In Langmuir–Blodgett films the dye molecules tend to reduce orientation freedom and strongly depend on surface morphology [28, 34, 35]. The silica network also restricts the rotation of dye molecules. Even the monodisperse R6G embedded in the silica glass cage is relocated around the Si–O–H bonds by hydrogen bonding [1].

Table 1 Spectroscopic parameters of R6G in various host environments

Host environment	$\lambda_{absorption}$ (nm)		$\lambda_{emission}$ (nm)
	$\lambda_{monomer}$	λ_{dimer}	
H_2O[a]	525	505	550
Ethanol[a]	531	505	558
SDS[b]	532	500	555[d]
Hydrophilic silica/water interface	530	495[c]	554
Hydrophobic silica/water interface	532	–	556
Toluene/water interface	536	–	557

[a] Govindanunny [42]
[b] Micheau et al. [43]
[c] Nasr [44]
[d] 1.0×10^{-6} M R6G and 0.1 mM SDS

In this measurement, the inner filter should be ruled out because of the low concentration of dye and the short light path of TIRF excitation, which just operates hundreds of nanometer.

The slight red shift of the fluorescent peak is independent of the concentration of R6G up to 1.0×10^{-6} M. Since the concentration range corresponds to the monolayer or sub-monolayer (compared with Ref [36]), no aggregates are expected. Prior studies on clay films [37], colloid spheres [33], and at the solid/air interface [36] were carried out at higher concentrations, where drastic red shifts caused by aggregates were observed with the increase of concentration. In our work, the spectra shifts could not be ascribed to the aggregation of the dye molecules on the solid substrate.

The slightly red shift (~5 nm) of fluorescence maxima of R6G at the silica /water interface, in comparison with those in the bulk, is mainly due to the interaction of substrate and dye. The limitation of rotational movements of the dye immobilized on the silica wall increases distinctly compared with the liquid counterpart. As shown in Fig. 4a and b, the polarized intensity of R6G at interface is different from that in water phase. At the interface, the vertical–vertical polarization increases in comparison to that in the bulk solution. The anisotropy measurements were carried out with four different combinations of horizontally and vertically polarized beams to the interface. The anisotropy at the interface was at least one order of magnitude increase in comparison with that in the bulk (r_{bulk}=0.015, $r_{interface}$= 0.16). The reorientation of R6G molecules at the interface substitutes the random alignment of dipole–dipole interaction between molecules in bulk phase. The interaction between Si–O–H at silica surface and dye decreases the

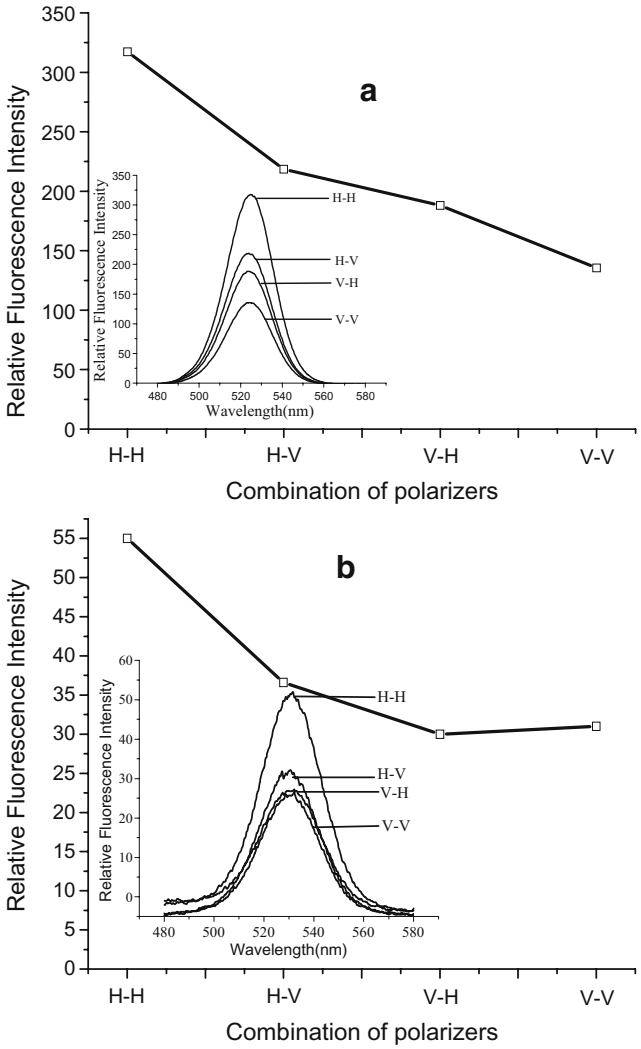

Fig. 4 Polarized synchronous fluorescence intensity of absorbed R6G: **a** in the aqueous solution at 525 nm; **b** at the silica/water interface at 530 nm. Vertical and horizontal polarizations are represented by V and H and combination of the polarizers by the pair of V and H for excitation-detection polarizers. [R6G]=5.0×10^{-7} M, PBS 7.4

dipole moment of the excited molecule [38], and hence the red shift may reflect the desired stabilizing mutual reorientation for the restricted motion of the dye around silica wall [1]. The rigidity of the silica surface restricts the freedom of the molecules.

The variation of local environment may also make a contribution to the phenomenon. It is found that the maximum absorption wavelength at interfaces (liquid/liquid, hydrophobic or hydrophilic solid/liquid) is longer than the corresponding wavelength in aqueous solution, close to the absorption wavelengths in the organic media or surfactants (Table 1). Similar situation exists for emission wavelengths. Polarity of microenvironment at the silica/water interface is lower than that in aqueous environment. The dye molecules are adsorbed to the silica wall, which is made up of two types of silicon groups: Si–O–H and Si–O–Si. Both groups are of lower polarity and higher hydrophobicity than water [1].

The adsorption behaviors of R6G with concentrations

The adsorption behaviors are affected by the concentration of R6G. As seen in Fig. 5, it is noticeable that the decrease of the bulk fluorescence intensity in evolution curves slows down with the increase of concentration; the interfacial signal rises up slowly. However, the interfacial fluorescence intensity does not always increase with the evolution of time: the curve reaches maximum in fluorescence intensity and then decreases at 5.0×10^{-7} M (Fig. 5b2) and 1.0×10^{-6} M (Fig. 5b3), while keeping obviously sustaining increase of interface intensity at the concentration of 1.0×10^{-7} M (Fig. 5b1). The increase of absorption (not show herein) confirmed the increasing amount of adsorbate at the interface, but no corresponding increase was found in fluorescence. It is suggested that the increasing concentration of bulk solution makes the shorter distance of dye molecules each other; therefore, resonant energy transfer deactivates the donors [27]. The differences among the evolution curves can be the result of self-quenching, which is due to interaction between close pairs of dye molecules at the high surface concentration.

The pH dependence of fluorescence intensity at the interface

Rhodamine B (RB) was chosen by Watarai et al. [39] as the target molecule at the interface since it is sensitive to the polarity of environment. However, the phenylcarboxyl group of RB makes it not a good model to probe the change of molecular conformation in the interface region, because the emission of RB is affected by the protonated form and the zwitterion form. In bulk solution, fluorescence intensity of R6G is not sensitive to pH. Harata et al. [6] studied the effect of subphase acidity at air/water interface on fluorescence signal and found that the fluorescence intensity of R6G at the interface changes in three steps by using confocal fluorescence microscope. This work confirms the pH-dependent character at the silica/water interface (Fig. 6a).

Constant fluorescence intensity was observed in the bulk solution at pH 1–5 and the intensity decreased when pH lower than 1 (Fig. 6b) It is evident that when pH<1, a portion of R6G molecules are protonated to form RH^{2+}, which results in an intense decrease in bulk fluorescence intensity. When pH>1, the cationic form R^{+} exists in the bulk solution.

For the surface observation, the intensity at the silica/water interface kept constant with pH 0–2 and increased

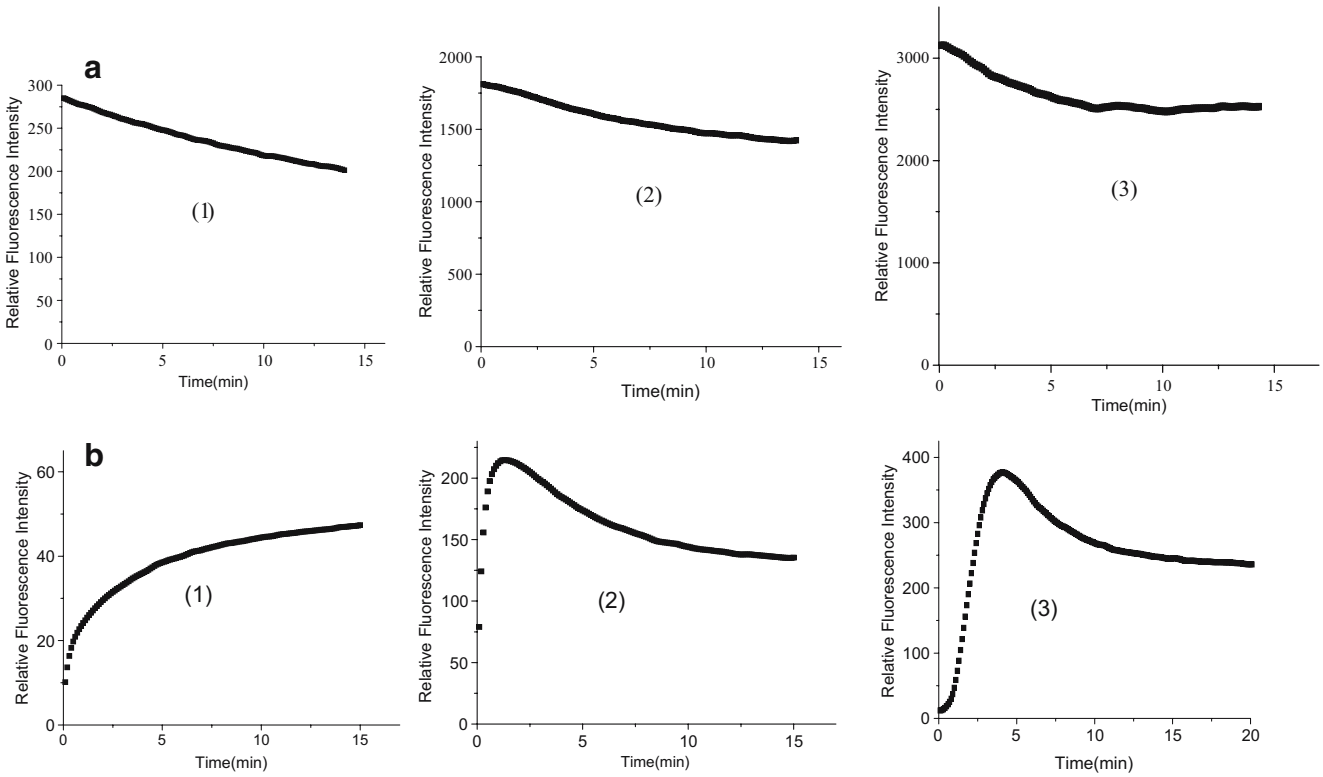

Fig. 5 The synchronous fluorescence intensity of R6G evolution curves with time **a** in aqueous solution at 525 nm, **b** at silica/water interface at 530 nm, for various concentrations of R6G in the bulk water phase: *1* 1.0×10^{-7} M, *2* 5.0×10^{-7} M, *3* 1.0×10^{-6} M. PBS 7.4

with the increasing pH from 2–5. Harata et al. [6] supposed a possibility to explain the acidity dependence that the chemical forms at the air/water interface change from RH^{2+} to R^+ to dimer or R^+–A^+ and they have different quantum yields. This hypothesis performs an incompetent role in the solid/liquid interface experiment. The charge at the silica surface will be the definitive factor in this case. Therefore, it is difficult to explain the analogous phenomena by the lower quantum yield of protonated molecules (RH^{2+}) or higher quantum yield of dimer/ R^+–A^+. If the quantum yield of molecule at the interface is kept stable as that in the bulk phase, it can be speculated that at the beginning the dye molecules adsorbed randomly at the interface; 10 min later, they reached to the equilibrium. The dependence of the fluorescence intensity at the interface on pH can reveal the equilibrium shift of the surface charge with subphase pH, which influences the interaction between the positively charged dye and the silica surface. The silica surface charged positive at pH 0–1 (isoelectric point=2.0) [40]. It is possible that the positive-charged monoethylamino group of R6G (RH^{2+} and R^+) is located at surface of silica randomly. Both RH^{2+} and $R^+$are repulsed by the positive-charged silica surface, so the relative weak fluorescence is detected. When pH increasing from 2 to 5, $R^+$is the dominant form in the solution (the contribution of RH^{2+} can be ignored). The adsorption of R^+ depends on the charge at silica surface which holds different negative charge at different pH. And less protonated silica surface can promote more adsorbate to adsorb at the interface.

Effect of ionic strength on fluorescence intensity of R6G

The ionic strength affects the adsorption behavior strongly at the interface. Some authors [10, 41] have found that supporting electrolyte influences the adsorption/desorption rates at surfaces. The adsorption of R6G at the silica/water interface in the absence of NaCl (Fig. 5b1) has an apparent difference in rates with the presence of NaCl: a fast initial adsorption event followed by a significant slower step. However, when 0.1 M NaCl (Fig. 7) exists in the bulk solution, the slow adsorption step is suppressed by the electrostatic interaction between adsorbate and surface.

Not only is the adsorption rate of R6G affected by the ionic strength, but also by the amount of adsorbate. Figure 8 shows the fluorescence intensities of dyes (1.0×10^{-7} M R6G) at the silica/water interface observed by TIRSF and in the bulk solution as a function of NaCl concentrations. The completely opposite trends are observed in the bulk and interface. In the bulk solution, NaCl causes a slight fluorescence increase. The impact hardly continues when more than 0.1 M NaCl is present in solution. The addition of NaCl results in the decrease in fluorescence intensity of

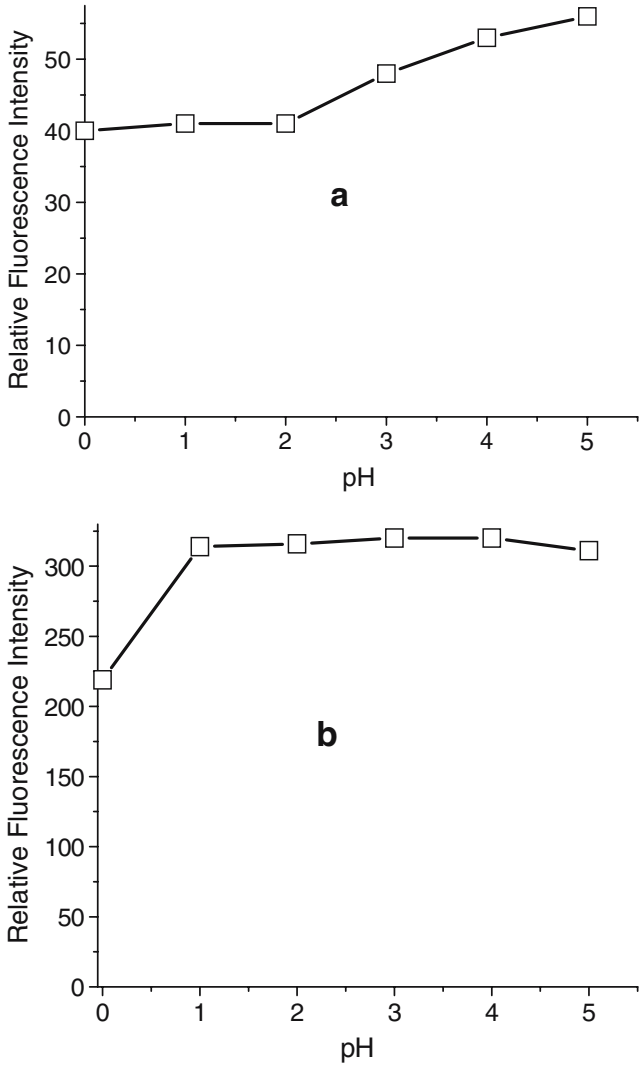

Fig. 6 Dependence of synchronous fluorescence intensity of R6G on pH **a** at the silica/water interface at 530 nm, **b** in the aqueous solution at 525 nm. [R6G]=1.0×10^{-7} M, [NaCl]=0.1 M

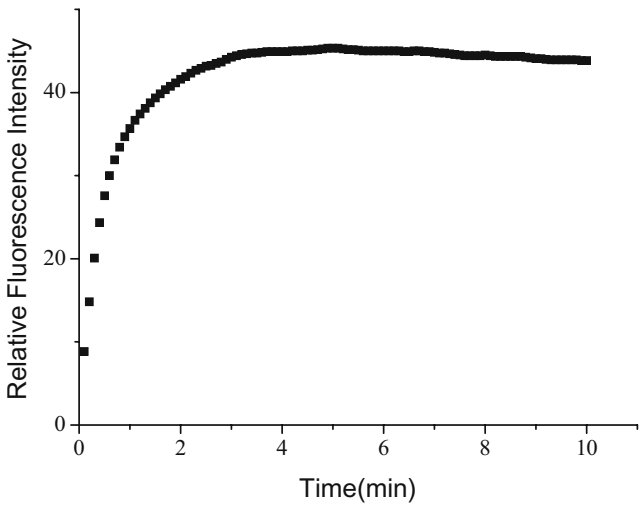

Fig. 7 R6G evolution curves of the fluorescence intensity with time at the interface in the presence of electrolyte. [R6G]=1.0×10^{-7} M, [NaCl]=0.1 M

R6G at the interface; the more salt is added, the lower interface intensity is observed, though the effect becomes weaker in high salt concentration range. Considering that NaCl can stabilize the interface fluorescence quickly, it is deduced that the change of the structure of electric double layer near silica substrate contributes to the decrease of adsorption of the fluorophore.

The cationic form of R6G (R^+) at neutral pH can neutralize the negative charged silica surface, which forms compact layer of electric double layer. Na^+ with less steric hindrance competes with R^+ to occupy the site of compact layer. As a result, a new buildup of electric double layer appears: Na^+ replaces R^+ to be another counterion to comprise compact layer and reduces the amount of adsorbed R6G. Therefore, it is reasonable that the fluores-

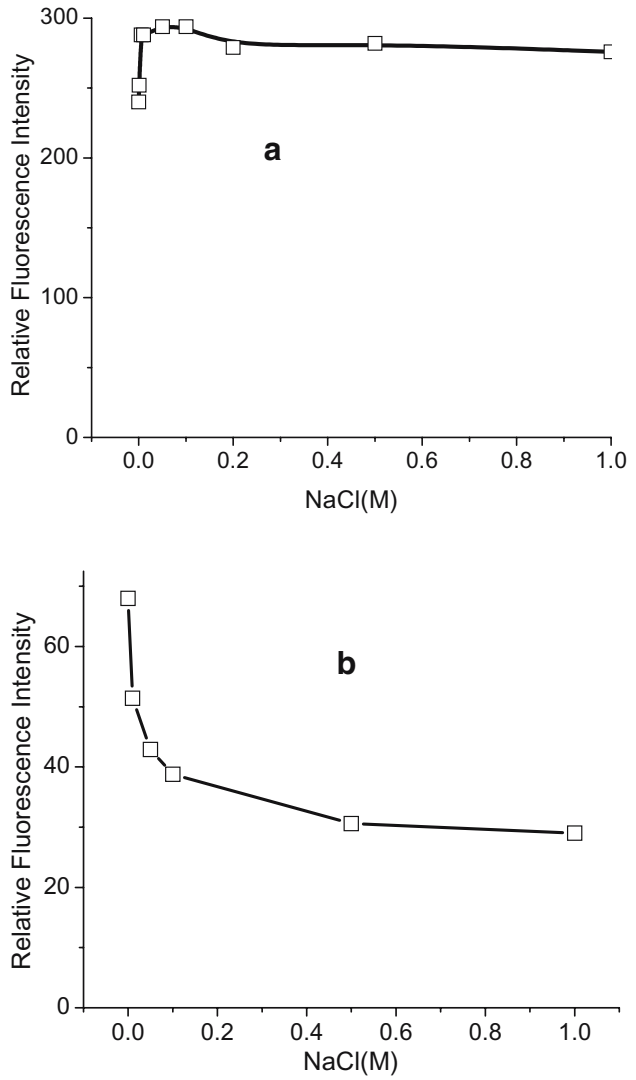

Fig. 8 The influence of ionic strength on the R6G **a** in the aqueous solution at 525 nm, **b** at the silica/water interface at 530 nm. [R6G]= 1.0×10^{-7} M

cence is weakened at the silica/water interface by the addition of NaCl.

In order to confirm this assumption, the effect of ionic strength on the hydrophobic modified silica/water in the interface is studied. Although just hydrophobic force drives the dye molecules adsorbing to the interface, more amounts of R6G molecules adsorb to the hydrophobic silica surface compared with the hydrophilic silica surface. The fluorescence on the hydrophobic silica/water interface, where the repulsion of electric double layer can be ignored, is not affected by the addition of salt (figure not shown here).

Conclusions

In this work, TIRSF is developed as a direct and successful tool to investigate the xanthene dye (R6G) at the silica/water interface. From analysis of fluorescence spectra both in the bulk and at the interface, it is clear that the characteristics of interface spectra are affected by more factors than previous reports.

Different from most of work on R6G in clay, nanoparticles, liquid crystal or sol–gel films as well as air–water interface, which obtains blue-shifted H-dimer or red-shifted J-dimer spectra of R6G on matrices, in this study, red shifts of fluorescence spectra at hydrophilic silica/water interface (5 nm, or 7 nm for hydrophobic, or 11 nm for toluene/water interface) are observed. This red shift is independent of the increase of the concentration of R6G solution. The bathochromic shift is mainly due to the limitation of rotational movements of the dye. The rigidity of the silica surface restricts the freedom of the molecules. The lower polarity of microenvironment at the silica/water interface than that in aqueous environment should also make a contribution to the phenomenon.

The adsorption of R6G at the silica/water interface depends on the concentration of bulk solution. With the increase of concentration, the decline tendency of the bulk fluorescence with time in evolution curves slowed down; the interfacial fluorescence signal rose up slowly. At 5.0×10^{-7} and 1.0×10^{-6} M, the decrease of the interfacial fluorescence after reaching the maximum is due to self-quenching of adsorbate.

The interfacial fluorescence intensity of R6G shows two steps change with pH: kept constant with pH 0–2 and increased with the increasing pH from 2–5, while the signal from the bulk solution keeps constant except a lower value at pH 0. The experimental results reveal the variances of both chemical forms of R6G and the equilibrium shift of the surface charge at the charged interface.

The adsorptive behaviors of adsorbate at silica/water interface depend on the ionic strength of dye solution as well. The structure of electric double layer affects the adsorptive rate and amount of R6G at the interface.

Acknowledgment This work was supported by the National Natural Science Foundation of China (29875023, 20575055) and the Natural Science Foundation of Fujian Province (B0410002).

References

1. Avnir D, Levy D, Reisfeld R (1984) The nature of the silica cage as reflected by spectral changes and enhanced photostability of trapped rhodamine 6G. J Phys Chem 88(24):5956–5959
2. Litwiler KS, Kluczynski PM, Bright FV (1991) Determination of the transduction mechanism for optical sensors based on rhodamine 6G-impregnated perfluorosulfonate films using steady-state and frequency-domain fluorescence. Anal Chem 63(8):797–802
3. Domenici C, Schirone A, Celebre M, Ahluwalia A, Rossi DD (1995) Development of a TIRF immunosensor: modelling the equilibrium behaviour of a competitive system. Biosens Bioelectron 10:371–378
4. Tapia Estevez MJ, Arbeloa FL, Arbeloa TL, Arbeloa IL (1993) Absorption and fluorescence properties of rhodamine 6G adsorbed on aqueous suspensions of Wyoming montmorillonite. Langmuir 9(12):3629–3634
5. Fang XH, Tan WH (1999) Imaging single fluorescent molecules at the interface of an optical fiber probe by evanescent wave excitation. Anal Chem 71(15):3101–3105
6. Zheng XY, Wachi M, Harata A, Hatano Y (2004) Acidity effects on the fluorescence properties and adsorptive behavior of rhodamine 6G molecules at the air–water interface studied with confocal fluorescence microscopy. Spectrochim Acta Part A 60:1085–1090
7. Zimadars D, Dadap JI, Eisenthal KB, Heinz TF (1999) Anisotropic orientational motion of molecular adsorbates at the air–water interface. J Phys Chem B 103(17):3425–3433
8. Polizzi MA, Plocinik RM, Simpson GJ (2004) Ellipsometric approach for the real-time detection of label-free protein adsorption by second harmonic generation. J Am Chem Soc 126 (15):5001–5007
9. Raschke MB, Hayashi M, Lin SH, Shen YR (2002) Doubly-resonant sum-frequency generation spectroscopy for surface studies. Chem Phys Lett 359:367–372
10. Hansen RL, Harris JM (1998) Measuring reversible adsorption kinetics of small molecules at solid/liquid interfaces by total internal reflection fluorescence correlation spectroscopy. Anal Chem 70(20):4247–4256
11. Yao MN, Li YQ (2004) Adsorption behavior of a water-soluble porphyrin at the glass-water interface as studied by synchronous total internal reflection fluorescence spectroscopy. Chin Chem Lett 15(1):109–111
12. Ghanadzadeh A, Zanjanchi MA (2001) Self-association of rhodamine dyes in different host materials. Spectrochim Acta Part A 57:1865–1871
13. Yamaguchi A, Kometani N, Yonezawa Y (2006) Phase and orientation control of mesoporous silica thin film via phase transformation. Thin Solid Films 513(1–2):125–135
14. Ma Z, Zaera F (2006) Organic chemistry on solid surface. Surf Sci Rep 61(5):229–281
15. Parida SK, Dash S, Patel S, Mishra BK (2006) Adsorption of organic molecules on silica surface. Adv Colloid Interface Sci 121:77–110
16. Martinez VM, Arbeloa FL, Prieto JB, Arbeloa IL (2005) Orientation of Adsorbed dyes in the interlayer space of clays. 1.

Anisotropy of rhodamine 6G in laponite films by vis-absorption with polarized light. Chem Mater 17(16):4134–4141
17. Tleugabulova D, Brennan JD (2006) Quantifying surface coverage of colloidal silica by a cationic peptide using a combined centrifugation/time-resolved fluorescence anisotropy approach. Langmuir 22(4):1852–1857
18. Matveeva E, Gryczynski Z, Malicka J, Gryczynski I, Lakowicz JR (2004) Metal-enhanced fluorescence immunoassays using total internal reflection and silver island-coated surfaces. Anal Biochem 334:303–311
19. Fujiwara N, Tsukahara S, Watarai H (2001) In situ fluorescence imaging and time-resolved total internal reflection fluorometry of palladium (II)-tetrapyridylporphine complex assembled at the toluene/water interface. Langmuir 17(17):5337–5342
20. Daly SM, Przybycien TM, Tilton RD (2005) Adsorption of poly (ethylene glycol)-modified lysozyme to silica. Langmuir 21 (4):1328–1337
21. Patra D, Mishra AK (2002) Recent developments in multicomponent synchronous fluorescence scan analysis. Trends in Anal Chem 21:787–798
22. Sui W, Wu C, Li YQ (2000) Rapid simultaneous determination of four anthracene derivatives using a single non-linear variable-angle synchronous fluorescence spectrum. Fresenius J Anal Chem 368:669–675
23. Lin DL, He LF, Li YQ (2004) Rapid and simultaneous determination of coproporphyrin and protoporphyrin in feces by derivative matrix isopotential synchronous fluorescence spectrometry. Clin Chem 50:1797–1803
24. Li YQ, Huang XZ, Xu JG (1999) Synchronous fluorescence spectrometric methodology in the wavelength domain. J Fluoresc 9(3):173–179
25. Li YQ, Xu JJ, Wang RT, Yu LJ, Li Z (2002) A spectrometric setup for synchronous total internal reflection fluorescence measurement at the solid/liquid interface. Chin Chem Lett 13:571–572
26. He LF, Lin DL, Li YQ (2005) Micelle-sensitized constant-energy synchronous fluorescence spectrometry for the simultaneous determination of pyrene, Benzo[*a*]pyrene and perylene. Anal Sci 21:641–645
27. Imhof A, Megens M, Engelberts JJ, de Lang DTN, Sprik R, Vos WL (1999) Spectroscopy of fluorescein (FITC) dyed colloidal silica spheres. J Phys Chem B 103(9):1408–1415
28. Ballt P, Auweraer MV, Schryver FCD (1996) Global analysis of the fluorescence decays of *N*, *N*'-Dioctadecyl rhodamine b in Langmuir-blodgett films of diacylphosphatidic acids. J Phys Chem 100(32):13701–13715
29. Arbeloa FL, Martinez VM (2006) Orientation of adsorbed dyes in the interlayer space of clays. 2 fluorescence polarization of rhodamine 6G in laponite films. Chem Mater 18(6):1407–1416
30. McRae EG, Kasha M (1964) Physical process in radiation biology. Academy Press, New York
31. Arbeloa L (1980) Fluorescence quantum yield evaluation: corrections for re-absorption and re-emission. J Photochem 31A:97–105
32. Pereira RV, Gehlen MH (2006) Spectroscopy of auramine fluorescent probes free and bound to poly(methacrylic acid). J Phys Chem B 110(13):6537–6542
33. Monte FD, Levy D (1999) Identification of oblique and coplanar inclined fluorescent J-dimers in rhodamine 110 doped sol–gel-glasses. J Phys Chem B 103(38):8080–8086
34. Ray K, Nakahara H (2002) Adsorption of sulforhodamine dyes in cationic Langmuir–Blodgett films: spectroscopic and structural studies. J Phys Chem B 106(1):92–100
35. Zhang ZJ, Nakashima K, Verma AL, Yoneyama M, Iriyama K, Ozaki Y (1998) Molecular orientation and aggregation in mixed Langmuir–Blodgett films of 5-(4-*N*-Octadecylpyridyl)-10,15,20-tri-*p*-tolylporphyrin and stearic acid studied by ultraviolet-visible, fluorescence, and infrared spectroscopies. Langmuir 14(5):1177–1182
36. Kikteva T, Star D, Zhao ZH, Baisley TL, Leach GW (1999) Molecular orientation, aggregation, and order in rhodamine films at the fused silica/air interface. J Phys Chem B 103(7):1124–1133
37. Martinez VM, Arbeloa FL, Prieto JB, Arbeloa IL (2005) Characterization of rhodamine 6G aggregates intercalated in solid thin films of laponite clay. 2. Fluorescence spectroscopy. J Phys Chem B 109(15):7443–7450
38. Bell JE (1981) Spectroscopy in biochemistry. CRC Press, Florida
39. Watarai H, Funaki F (1996) Total internal reflection fluorescence measurements of protonation equilibria of rhodamine B and octadecylrhodamine B at a toluene/water interface. Langmuir 12 (26):6717–6720
40. Perk GA (1965) The isoelectric points of solid oxides, solid hydroxides, and aqueous hydroxo complex systems. Chem Rev 65 (2):177–198
41. Waite SW, Holzwarth JF, Harris JM (1995) Laser temperature jump relaxation measurements of adsorption/desorption kinetics at liquid/solid interfaces. Anal Chem 67(8):1390–1399
42. Govindanunny T (1980) Solvation effects on the tunability of a fluorescein dye laser. Appl Phys 23:253–258
43. Micheau JC, Zakharova GV, Chibisov AK (2004) Reversible aggregation, precipitation and re-dissolution of rhodamine 6G in aqueous sodium dodecyl sulfate. Phys Chem Chem Phys 6:2420–2425
44. Nasr C, Liu D, Hotchandani S, Kamat PV (1996) Dye-capped semiconductor nanoclusters. Excited state and photosensitization aspects of rhodamine 6G H-aggregates bound to SiO_2 and SnO_2 colloids. J Phys Chem 100(26):11054–11061